AD_____

CONTRACT NO: DAMD17-91-C-1058

TITLE: ANALYSIS OF STRUCTURE AND SPECIFIC FUNCTIONAL
                  GROUPS INVOLVED IN ACETYLCHOLINESTERASE CATALYSIS
                  AND INHIBITION

PRINCIPAL INVESTIGATOR: Palmer Taylor, Ph.D.

Contracting Organization: University of California, San Diego
                             Department of Pharmacology
                             La Jolla, CA 92093-0636

REPORT DATE: October 1, 1994

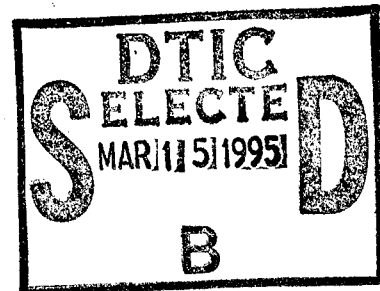TYPE OF REPORT: Final Report

PREPARED FOR:

    U.S. ARMY MEDICAL RESEARCH AND MATERIEL COMMAND
    FORT DETRICK
    FREDERICK, MARYLAND 21702-5012

DISTRIBUTION STATEMENT: Approved for public release;
                             distribution unlimited

19950314 143

DTIC
SELECTED
MAR 15 1995
B

DTIC QUALITY INSPECTED 1

REPORT DOCUMENTATION PAGE

Public reporting burden for this collection of information is estimated to average 1 hour per response, including the time for reviewing instructions, searching existing data sources, gathering and maintaining the data needed, and completing and reviewing the collection of information. Send comments regarding this burden estimate or any other aspect of this collection of information, including suggestions for reducing this burden, to Washington Headquarters Services, Directorate for Information Operations and Reports, 1215 Jefferson Davis Highway, Suite 1204, Arlington, VA 22202-4302, and to the Office of Management and Budget, Paperwork Reduction Project (0704-0188), Washington, DC 20503.

1. AGENCY USE ONLY (Leave blank)	2. REPORT DATE 1 Oct. 94	3. REPORT TYPE AND DATES COVERED FINAL 6/14/91 – 9/13/94

4. TITLE AND SUBTITLE
ANALSIS OF STRUCTURE AND SPECIFIC FUNCTIONAL GROUPS
INVOLVED IN ACETYLCHOLINESTERASE CATALYSIS AND INHIBITION

5. FUNDING NUMBERS
Contract No.
DAMD17-91-C-1058

6. AUTHOR(S)

PALMER TAYLOR

7. PERFORMING ORGANIZATION NAME(S) AND ADDRESS(ES)

University of California, San Diego
Department of Pharmacology
La Jolla, California 92093-0636

8. PERFORMING ORGANIZATION REPORT NUMBER

9. SPONSORING/MONITORING AGENCY NAME(S) AND ADDRESS(ES)

U.S. Army Medical Research and Materiel Command
Fort Detrick
Frederick, Maryland 21702-5012

10. SPONSORING/MONITORING AGENCY REPORT NUMBER

11. SUPPLEMENTARY NOTES

12a. DISTRIBUTION/AVAILABILITY STATEMENT

Approved for public release; distribution unlimited

12b. DISTRIBUTION CODE

13. ABSTRACT (Maximum 200 words)

The interactions of substrates, inhibitors and antibodies with *Torpedo* and mammalian acetylcholinesterases and butyrylcholinesterases have been studied by enzyme kinetic analyses, site-specific mutagenesis, molecular modeling, and peptide and antibody titrations. The high yield expression systems we developed have enabled us to obtain sufficient wild-type and mutant enzymes for the kinetic and physical studies. These studies have benefited from the availability of a three-dimensional X-ray-derived structure of acetylcholinesterase which allows for interpretations at an atomic level of resolution. Three distinct regions in the enzyme appear responsible for conferring selectivity: the acyl pocket defined primarily by phenylalanines 295 and 297, the choline subsite primarily defined by tryptophan 86, tyrosine 337 and glutamate 202 and the peripheral anionic site defined by tryptophan 286, tyrosine 72, tyrosine 124 and aspartate 74. Through site-specific mutagenesis we have been able to modify acyl pocket specificity, selectivity toward neutral and charged substrates, substrate inhibition, organophosphate reactivity, organophosphate aging and oxime reactivation. These studies have important implications in developing superior antidotes for organophosphate poisoning and in using recombinant acetylcholinesterase as an antidote.

14. SUBJECT TERMS
Enzymes, Genetic Engineering, Acetylcholinesterase

15. NUMBER OF PAGES

16. PRICE CODE

17. SECURITY CLASSIFICATION OF REPORT	18. SECURITY CLASSIFICATION OF THIS PAGE	19. SECURITY CLASSIFICATION OF ABSTRACT	20. LIMITATION OF ABSTRACT
Unlimited	Unlimited	Unlimited	Unlimited

NSN 7540-01-280-5500

Standard Form 298 (Rev 2-89)
Prescribed by ANSI Std Z39-18
298-102

FOREWORD

Opinions, interpretations, conclusions and recommendations are those of the author and are not necessarily endorsed by the U.S. Army.

(X)   Where copyrighted material is quoted, permission has been requested to use such material.
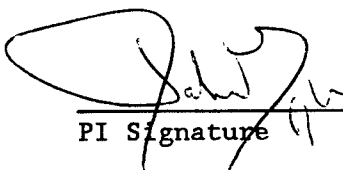
(NA)   Where material from documents designated for limited distribution is quoted, permission has been obtained to use the material.

(X)   Citations of commercial organizations and trade names in this report do not constitute an official Department of the Army endorsement or approval of the products or services of these organizations.

(X)   In conducting research using animals, the investigator(s) adhered to the "Guide for the Care and Use of Laboratory Animals," prepared by the Committee on Care and Use of Laboratory Animals of the Institute of Laboratory Animal Resources, National Research Council (NIH Publication No. 86-23, Revised 1985).

(NA)   For the protection of human subjects, the investigator(s) have adhered to policies of applicable Federal Law 45 CFR 46.

(X)   In conducting research utilizing recombinant DNA technology, the investigator(s) adhered to current guidelines promulgated by the National Institutes of Health.

_____   10/1/94

PI Signature   Date

ii

Accession For

NTIS GRA&I	☑
DTIC TAB	☐
Unannounced	☐
Justification	

By_____
Distribution/_____

Availability Codes

Dist	Avail and/or Special
A-1	

TABLE OF CONTENTS

Analysis of Structure and Specific Functional Groups Involved in
Acetylcholinesterase and Inhibition

List of Figures and Tables

INTRODUCTION

This project began in 1991 at a time when we had available sequences of both *Torpedo* and mammalian acetylcholinesterase (AChE), but before the crystal structure was published (1). Solving the crystal structure enabled us and other groups to extend our interpretations to an atomic level of resolution. As noted below this development also changed the emphasis of some of the specific aims. The early years of our DAMD contract supported the initial cloning of *Torpedo* AChE (2), determination of its disulfide bonding pattern (3), identification of the active center peptide (4) and ascertaining the divergences in primary structure of the alternatively spliced forms of *Torpedo* AChE (5). The primary structure served as the template for aligning the amino acids and disulfide linkages in the first crystal structure, which was solved by Joel Sussman and Israel Silman and their colleagues at the Weizmann Institute (1). Our initial mutagenesis work occurred prior to a high-resolution crystal structure (6), but nevertheless uncovered the importance of the E_{199} mutant and established that H_{440} was the catalytic triad.

In 1990 our interests turned to the mammalian enzymes, and the cloning of mouse AChE cDNA (7) provided the first report of a full mammalian AChE structure. Subsequent genomic cloning helped resolve the gene structure and splicing patterns for both mouse and human AChE, MAChE and HChE, respectively (8) and factors regulating gene expression (9-11). Studies supported by the DAMD contract have been mainly directed toward AChE structure-function relationships using site-specific mutagenesis, kinetic characterization of the mutant enzymes, protein chemistry, site-directed labeling and antibody techniques. The primary emphasis has been on mutagenesis and expression, and we detail below our progress from 1991 to present:

BODY

[Note that the references to our work are labeled as 1P-19P since they denote publications of work or reviews of work specifically supported by this contract]

Our past contract had three distinct objectives: The first was directed to locating discrete functional regions in AChE by protein modification and then ascertaining function through site-specific mutagenesis. Fortunately the completion of a three-dimensional (3-D) structure of AChE (1) and certain of its ligand complexes (12) made residue location by chemical modification somewhat redundant and enabled us to proceed directly to site-specific mutagenesis. The influence of the mutation on a particular function allowed one to confirm location. In particular, aims 1b and 1c in the previous proposal were not pursued by chemical modification but rather by examining the role played by residues in the active center through site-specific mutagenesis. The added value of the mutagenesis approach is that it permitted us to partition free energy of interaction (ΔG) to particular side chains and ascertain how the residues function in conferring substrate inhibition or activation as well as influencing ligand specificity at the active center and peripheral site. In short, we have defined the domains of the peripheral site regions of alkylphosphate association and regions that would be labeled by the acetylcholine mustard, bifunctional alkylphosphates and onchidal. Hence, an alternative and more efficient approach was utilized to satisfy aims 1b and 1c and to extend these concepts beyond the initial objectives.

A. **Expression Studies**

Our initial transient transfections yielded only small quantities of enzyme and required quantitation by antibody (3P). Over the project period we sought improvements in expression, and our alternative approaches are detailed below.

1. <u>Transient Transfections</u>: We have used $Ca_3(PO_4)_2$, DEAE-Dextran, liposome-based systems and electroporation for transfection. While certain specialized cell lines have proven nearly intractable for transfection by $Ca_3(PO_4)_2$, in our hands this method has been most satisfactory in SV-40-based COS cells or CMV-based transfections into monkey kidney (COS), human embryonic kidney (HEK), baby hamster kidney (BHK) and

Chinese hamster ovary (CHO) cells. The cytomegalovirus (CMV) expression system gives the greatest expression. BHK cells grow more rapidly than HEK cells, but do carry small quantities of endogenous butyrylcholinesterase (BuChE) activity.

2. <u>Permanent Transfectants</u>: Virtually all of the mouse mutations described herein now exist as permanent transfectants in stock cultures. Selection is based on neomycin resistance achieved by cotransfection of a neomycin acetylation gene. In most cases the "neo-resistant" colonies are few and we have not subcloned them. The soluble or secreted form of the enzyme is expressed for studies of catalytic mechanism. AChE activities range up to 30 Units or 1 μg per 10 cm plate.

3. <u>Baculovirus Expression</u>: Several of the *Torpedo* mutants and wild-type enzyme and a few of the mouse constructs have been placed behind the P-12 or polyhedron promoter in the baculovirus vector and the viral stocks cloned. The larger viral vector, the requirements for recombination in the cells after infection and cloning the recombinants, the stability of the virus and the necessity of maintaining separate culture conditions for the *Spodoptera* Sf-9 cells combine to make this a fairly labor-intensive endeavor. New vectors and selection procedures developed over the last few years have reduced the time requirements somewhat. We have been able to obtain up to 3 mg (90 Units) per liter of serum-free culture media or per 4×10^9 cells (a typical density of suspensions). The expressed enzymes have been purified to homogeneity (3P). Hence, baculovirus-based systems remain necessary for high expression of the membrane-associated forms of *Torpedo* and mammalian AChE. Our baculovirus expressed *Torpedo californica* mutants at E_{199} are being studied with various inhibitors by Dr. Donald M. Maxwell at Edgewood, Dr. B.P. Doctor at Walter Reed and by Dr. Daniel Quinn at Iowa.

4. <u>Glutamine Synthetase Amplication Vectors and Chinese Hamster Ovary (CHO) Cell Expression</u>: A recent innovation has been the employment of glutamine synthetase (GS) gene amplification for expression of secreted enzyme (i.e., soluble or hydrophilic AChE or BuChE). The system relies on coexpression of the gene of interest (*AChE* or *BuChE*) behind a CMV promoter in a vector containing the *glutamine synthetase* (*GS*) gene. Selection and maintenance of cells is done in glutamine-free media containing methionine sulfoximine (a GS-inhibitor). Only cells producing large quantities of GS (resulting from gene amplification) survive. Although we have been unsuccessful in obtaining permanent transfectants with the GS selection system for BHK or HEK cells, the CHO system has yielded surprising results. These cells grow well on large plates or in roller bottles in serum-free medium and continue to secrete cholinesterase after achieving confluence. Gene amplification yields far higher expression. A single roller bottle produces 500 μg of AChE every 3 days in a 50 ml volume and this continues for over a month!

This expression system is a marked improvement on baculovirus-*Spodoptera* or embryonic kidney cells for secreted enzyme and has become our method of choice for production of recombinant enzyme to study catalytic and inhibition parameters. At our suggestion other groups whose work is supported by DAMD contracts also now employ this expression system.

B. **Identification of Antibody Recognition Sites on Acetylcholinesterase**

The original AChE monoclonal antibodies were produced by B.P. Doctor while on sabbatical at UCSD. His group has carried the lead in generation of new antibody families and their characterization. Our role has been in ascertaining epitopes to some of the antibodies. Our first study with synthetic peptides distinguished exposed from buried epitopes within the active center gorge and their disposition with respect to the active center peptide (1P). The second study identified the epitopes for two monoclonal antibodies (7P). One, 4E-7, is directed to an oligosaccharide, and we identified the conjugated carbohydrate at Asn 59 as its epitope. The second antibody, 2C-9, does not depend on an oligosaccharide but rather recognizes a peptide sequence between residues 47 and 59. These regions are close to one another in the 3-D structure, exposed on the surface and encompass a major antigenic area peripheral to

2

the active center. The position of this region within the 3-D AChE structure lies on the back surface away from the active center gorge.

Fig. 1. Stereoscopic view of 3-D structure of *Torpedo* AChE. The synthetic antigenic peptide, residues 44-63, is shown as a ribbon structure. The locations of side chains for the active site Ser^{200}, for His^{400}, which particpates in the catalytic triad, and for Trp^{84}, which stabilizes the choline moiety in acetylcholine are also indicated. Coordinates were provided by J. Sussman, and the images are generated by Biosym Insight II program using the Silicon Graphics Personal Iris 4D/35 system.
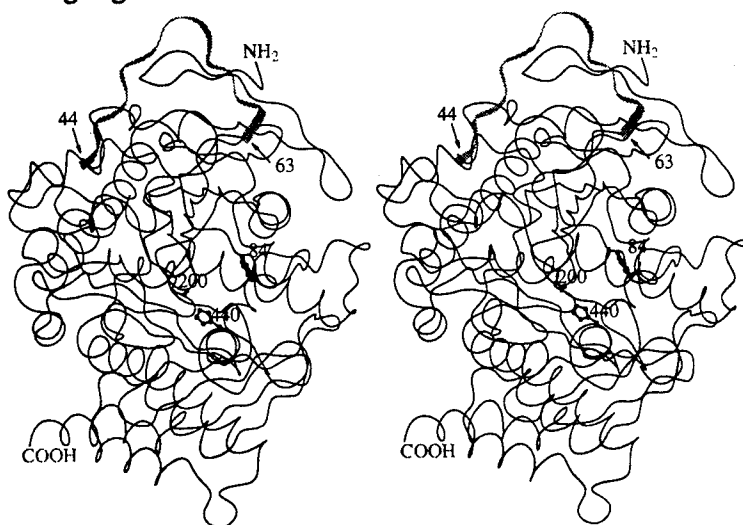
C. Structure-Activity Analysis by Mutagenesis

In our view, the study of mutant cholinesterases should have a twofold objective, first to identify functionally important residues and second to uncover details of enzyme mechanism. The latter goal requires a detailed kinetic analysis rather than simply a survey of the activity of the mutants. Certain minimal criteria are necessary to enable one to relate kinetic or equilibrium data to structure and correlate findings between laboratories.

First, substrate inhibition or activation should be analyzed in terms of a four-parameter equation, K_m, k_{cat}, K_{ss} and b, where K_m and k_{cat} are the normal Michaelis-Menten constants, K_{ss} is the dissociation constant for binding of the second substrate molecule and b is the ratio of efficiencies of catalysis of the SES (substrate inhibited) and ES complexes. Curve fitting over a large range in concentrations is the optimal means for parameter estimation and minimizing an error bias.

Second, AChE expression should be sufficient to titrate active sites in order to determine k_{cat} accurately. High expression is also necessary for measurements at high substrate concentration (up to 100 μM) for determining K_{ss}.

Third, inhibition mechanisms should be analyzed so that inhibition of the same species of enzyme (E, ES or acylated enzyme) is being compared in the mutant and wild-type enzyme.   Values such as IC$_{50}$, which are dependent on substrate K_m's (depending on the competitive and noncompetitive components), are of limited value for interpretation. Moreover, they do not distinguish the enzyme species (E, ES or acylated enzyme) with which inhibition is taking place. Irreversible inhibitors should also be analyzed in terms of rate and equilibrium constants rather than IC$_{50}$'s.

Fourth, the influence of side chain substitutions should be analyzed in terms of free energy differences, $\Delta\Delta G$, rather than dissociation constants. Protein structures and their ligand-complexes are energy-minimized, and similar units should apply to the binding or catalytic parameters. These principles are applied in references 3P, 4P, 5P and 6P.

D. Studies on Enzyme Structure with Mutagenesis [In this and other sections, numbering of residues corresponding to the mammalian sequences will be generally used. In the cases where the *Torpedo* system was studied, the numbers will be noted in parentheses].

1. The Choline Binding Subsite of the Active Center

(a) *Electrostatic Involvement*: During this project period we followed up in detail our early observation that the glutamate amino-terminal to the catalytic serine (E_{199}) affected catalysis. To this end we expressed large quantities of the mutant enzymes $E_{(199)}Q$, $E_{(199)}D$ and examined substrate and inhibitor binding kinetics (3P). Several important concepts emerged:

(1) Loss of the charge on E_{199} reduces k_{cat}/K_m to about 2% of wild-type enzyme (Table I) (3P).

(2) Altering the position of the residues in the catalytic triad by removing a methylene group ($E_{(199)}D$) decreases k_{cat}/K_m to ~20% of the wild-type (Table I). More importantly, this substitution eliminates substrate inhibition (3P).

(3) Removal of the charge influences affects edrophonium binding to a greater extent than that for weaker inhibitors such as phenyltrimethylammonium (Table II).

Table I: Kinetic Parameters (±Standard Errors) for Wild-Type and Mutant Acetylcholinesterases Expressed in a Baculovirus–*Spodoptera* System[a]

enzyme	$10^3 K_m$ (M)	$K_{m\ wt}/K_{m\ mut}$	$10^3 K_{ss}$ (M)	$K_{ss\ wt}/K_{ss\ mut}$	$10^5 k_{cat}$ (min^{-1})	$10^9 k_{cat}/K_m$
Torpedo wild type (tissue derived)	0.076		25		2.5 ± 0.5	3.3
Torpedo wild type (recombinant)	0.048 ± 0.005	1	32 ± 3	1	1.5 ± 0.3	3.1
Torpedo Glu$^{199} \rightarrow$ Gln	0.66 ± 0.16	0.07	151 ± 18	0.2	0.42 ± 0.14	0.064
Torpedo Glu$^{199} \rightarrow$ Asp	0.043 ± 0.014	0.9	–	–	0.30 ± 0.13	0.7
mouse wild type	0.076 ± 0.012		25 ± 2		1.3 ± 0.1	1.7

[a] Kinetic constants were determined by measuring activity versus substrate concentration and fitting the curves according to eq 1. The dash indicates that no substrate inhibition was detected up to concentrations of 300 mM substrate. Mean values and standard errors for K_m and K_{ss} were determined by curve fitting to eq 1. Data come from three to eight experiments and three preparations of enzyme. k_{cat} was determined from measurements of V_{max} and titration of active site concentrations on three preparations of enzyme.

Table II: Reversible Inhibition of Torpedo Acetylcholinesterase

recombinant enzyme	K_i[a] ± standard error (μM)									
	propidium		edrophonium		phenyltrimethyl-ammonium		3-hydroxypyridine		3-hydroxy-*N*-methylpyridinium	
	comp	noncomp	comp	noncomp	comp	noncomp	comp	noncomp	comp	noncomp
wild type	0.35 ± 0.08	0.67 ± 0.08	0.23 ± 0.07	–	80	500	2.2×10^4	3.5×10^4	$6.3 \pm 0.9 \times 10^3$	$1.9 \pm 0.6 \times 10^4$
Glu$^{199} \rightarrow$ Gln	0.75 ± 0.35	–	5.7 ± 0.9	–	440	–	$4.8 \pm 0.7 \times 10^4$	$1.8 \pm 1.2 \times 10^5$	$1.2 \pm 0.8 \times 10^4$	1.6×10^4
Glu$^{199} \rightarrow$ Asp	4.5 ± 2.5	8.0	2.5 ± 1.5	–	50	–	3.3×10^4	–	nd	nd

[a] The dashes indicate that the constant for the other mode of inhibition was indeterminate or at least 10-fold greater than the paired constant determined for the specified mode of inhibition. nd, not determined. Inhibition was determined from reciprocal plots of velocity and substrate concentrations. Replots of the apparent K_m and V_{max} versus inhibitor concentration yielded the competitive and noncompetitive components. Standard errors are shown when separate preparations of enzyme were analyzed.

(4) Removal of the charge slows acylation more than deacylation rates for carbamoylating agents (3P) (Tables III & IV).

Table III: Progressive Inhibition of Recombinant Acetylcholinesterases[a]

| inhibitor | AChE | inhibition constants | | | k_a wt/k_a mut |
		K_a (M)	k_{+2} (min^{-1})	k_a (M^{-1} min^{-1})	
M7C	Torpedo wt	$(8.5 \pm 3.7) \times 10^{-6}$	5.8 ± 4.4	$(8.5 \pm 2.4) \times 10^5$	
	Torpedo Gln[199]	$(2.4 \pm 0.15) \times 10^{-5}$	1.1 ± 0.1	$(4.5 \pm 0.5) \times 10^4$	19
	Torpedo Asp[199]	$(8.7 \pm 2.4) \times 10^{-7}$	2.0 ± 0.4	$(2.4 \pm 0.2) \times 10^6$	0.4
	mouse	$(1.3 \pm 0.63) \times 10^{-6}$	5.3 ± 2.5	$(6.0 \pm 1.1) \times 10^6$	
eserine	Torpedo wt	–	–	$(1.1 \pm 0.24) \times 10^6$	
	Torpedo Gln[199]	9.0×10^{-6}	3.9	$(4.3 \pm 0.7) \times 10^5$	3
	Torpedo Asp[199]	5.6×10^{-6}	2.1	$(3.7 \pm 0.1) \times 10^5$	3
	mouse	–	–	$(8.5 \pm 0.8) \times 10^5$	
neostigmine	Torpedo wt	–	–	6.4×10^5	
	Torpedo Gln[199]	6.0×10^{-6}	0.57	9.5×10^4	7
	Torpedo Asp[199]	–	–	$(1.3 \pm 0.1) \times 10^5$	5
	mouse	–	–	5.7×10^6	
pyridostigmine	Torpedo wt	$(1.0 \pm 0.2) \times 10^{-4}$	0.17 ± 0.003	$(2.0 \pm 0.44) \times 10^3$	
	Torpedo Gln[199]	$(1.9 \pm 0.19) \times 10^{-3}$	0.18 ± 0.006	$(9.4 \pm 0.06) \times 10^1$	21
	Torpedo Asp[199]	$(6.3 \pm 1.8) \times 10^{-4}$	0.59 ± 0.03	$(1.0 \pm 0.3) \times 10^3$	2
	mouse	9.5×10^{-6}	4.6	4.9×10^5	

[a] Enzyme inhibition was measured in 0.1 M NaPO$_4$, pH 7.0, as a function of time and inhibitor concentration. At least three inhibitor concentrations were used. Kinetics were analyzed   Where the dashes are shown, the rates were too rapid to ascertain K_a and k_2 by conventional mixing techniques. Standard errors are shown in the cases where determinations were made on two or more preparations.

Table IV: Spontaneous Reactivation of Recombinant Acetylcholinesterase

$$EA \xrightarrow[H_2O]{k_{+3}} E + A$$
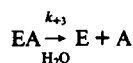
inhibitor[a]	AChE	$10^3 k_{+3}$[b] (min^{-1})	k_{+3} wt/k_{+3} mut
M7C	Torpedo wt	1.6 ± 0.12	
	Torpedo Gln[199]	0.58 ± 0.27	3
	Torpedo Asp[199]	1.2 ± 0.35	1
	mouse	1.9	
eserine	Torpedo wt	5.4 ± 1.2	
	Torpedo Gln[199]	1.5 ± 0.1	4
	Torpedo Asp[199]	1.4 ± 0.22	4
	mouse	8.1	
pyridostigmine	Torpedo wt	1.5 ± 0.30	
	Torpedo Gln[199]	0.86 ± 0.47	2
	Torpedo Asp[199]	nd[c]	
	mouse	2.3	

[a] AChE was initially inhibited ~80–90% with listed inhibitors. Return of enzyme activity was monitored as a function of time upon 1000-fold dilution of inhibition mixture. No reactivation was detected for methanesulfonyl fluoride or haloxon inhibition. [b] Standard errors are shown when measurements were made on multiple enzyme preparations. [c] Not determined.

5

(5) The charge is also critical to phosphorylation rates as the $E_{(199)} \to Q$ mutation shows a reduction of inhibition by DFP and other alkylphosphates by two orders of magnitude (3P). It also affects the rates of enzyme aging (8P - see specific aims). (Table V)

Table V: Inhibition of Recombinant Native and Mutant Acetylcholinesterases by Organophosphates and Sulfonates

| inhibitor | AChE | inhibition constants[a] | | | k_a wt$/k_a$ mut |
		K_a (M)	k_{+2} (min^{-1})	k_a (M^{-1} min^{-1})	
haloxon	wt	$(1.4 \pm 0.45) \times 10^{-6}$	0.60 ± 0.4	$(4.7 \pm 1.8) \times 10^5$	
	Gln^{199}	$(2.2 \pm 0.67) \times 10^{-5}$	0.18 ± 0.012	$(9.4 \pm 0.24) \times 10^3$	50
	Asp^{199}	1.7×10^{-5}	1.6	$(8.0 \pm 1.2) \times 10^4$	6
	mouse	1.0×10^{-5}	2.5	2.5×10^5	
paraoxon	wt	$(5.8 \pm 1.1) \times 10^{-5}$	3.8 ± 1.2	$(7.7 \pm 1.6) \times 10^6$	
	Gln^{199}	$(7.3 \pm 4.7) \times 10^{-4}$	0.54 ± 0.23	$(9.3 \pm 2.8) \times 10^2$	83
	Asp^{199}	–	–	$(3.1 \pm 0.12) \times 10^4$	3
	mouse	2.7	9.0	1.5×10^6	
MEPQ	wt	–	–	$(2.9 \pm 0.45) \times 10^8$	
	Gln^{199}	–	–	9.6×10^6	30
	Asp^{199}	–	–	7.5×10^7	4
	mouse	–	–	1.3×10^8	
DFP	wt	–	–	$(1.0 \pm 0.19) \times 10^4$	
	Gln^{199}	$(8.0 \pm 1.5) \times 10^{-3}$	0.30 ± 0.05	$(3.8 \pm 0.8) \times 10^1$	263
	Asp^{199}	7.4×10^{-4}	1.6	$(1.8 \pm 0.35) \times 10^3$	6
	mouse	–	–	1.1×10^4	
methanesulfonyl fluoride	wt	–	–	2.2×10^2	
	Gln^{199}	–	–	4.7×10^1	5
	Asp^{199}	–	–	$(9.1 \pm 4) \times 10^1$	2
	mouse	–	–	2.9×10^2	

[a] Rates of inhibition were determined as described in Table III. Standard errors are shown when measurements were made on multiple enzyme preparations.

(6) Trifluoroketone transition state analogues yield new information on catalytic mechanism. In conjunction with a sabbatical visitor, Dr. Daniel Quinn, we examined the influence of charge on the association on trimethylammoniophenyl trifluoromethyl ketone, the primary, secondary and tertiary amine congeners and the uncharged m-isopentylphenyl trifluoromethyl ketone. Elimination of charge diminishes binding constants by a factor of 300 (~2.1 kcal), and this loss of free energy is identical irrespective of whether the charge is on the enzyme or the ligand. The affinities of these compounds are in the picomolar range, and kinetics are consistent with formation of a hemiketal conjugate with the enzyme.

(b) *Influence of Aromatic Groups*: We have mutated Y_{337} (which corresponds to F_{330} in *Torpedo* and A_{328} in BuChE) to A and find that this mutation replicates many of the AChE/BuChE specificity differences. This residue change has little effect on substrate catalytic parameters, and on the binding of tricyclic inhibitors such as tacrine, but it has a large influence on tricyclic inhibitors with large side chains such as ethopropazine (5P) (Tables VIa & b). In fact, ethopropazine's selectivity for BuChE is a consequence of the lack of steric interference of the diethylamino-isopropyl group on the phenothiazine with the aromatic side chain at the 337 position. By contrast, the aromatic residue at 337 is primarily responsible for huperzine's preference for AChE over BuChE (9P) (Tables VIIa & b). In each case, when we compare $\Delta\Delta G$ for the AChE/BuChE pair with the $Y_{337}A$ mutation, the correspondence is striking (5P,9P).

6

Table VIa Dissociation Constants[a] (μM) and Changes in Free Energy (ΔΔG) for Reversible Inhibition of Mouse Wild-Type and AChE Y_{337} Mutant Cholinesterases

	AChE wt		BuChE wt		$Y_{337}A$		$Y_{337}F$	
inhibitor	K_I	αK_I	K_I	αK_I	K_I	αK_I	K_I	αK_I
edrophonium	0.30 ± 0.10	6.4 ± 0.6	110 ± 37	1400 ± 700	5.6 ± 1.3	26 ± 14	0.29 ± 0.06	7.8 ± 0.8
acridine	6.1 ± 2.2	26 ± 7	1.6 ± 0.9	5.4 ± 3.6	0.87 ± 0.15	3.4 ± 0.8	20 ± 4	210 ± 22
N-methyl-acridininium	0.73 ± 0.19	1.2 ± 0.3	0.19 ± 0.05	0.29 ± 0.08	0.049 ± 0.010	0.13 ± 0.03	1.3 ± 0.3	7.8 ± 2.3
9-aminoacridine	0.040 ± 0.010	0.11 ± 0.03	0.022 ± 0.010	0.034 ± 0.013	0.0023 ± 0.0007	0.0059 ± 0.0010	0.171 ± 0.055	0.71 ± 0.15
tacrine	0.040 ± 0.010	0.13 ± 0.05	0.017 ± 0.004	0.047 ± 0.022	0.0015 ± 0.0005	0.005 ± 0.001	0.15 ± 0.03	0.68 ± 0.18
promazine	50 ± 10	790 ± 230	1.8 ± 0.7	7.1 ± 3.9	37 ± 11	150 ± 27	51 ± 12[b]	850 ± 21
chlorpromazine	26 ± 8	410 ± 290	2.1 ± 0.9	8.5 ± 4.0	17 ± 7	91 ± 38	22 ± 11[b]	540 ± 191
promethazine	230 ± 64	4100 ± 4100	1.4 ± 0.7	3.3 ± 0.2	29 ± 11	130 ± 29	110 ± 20	1700 ± 440
ethopropazine	110 ± 51	1100 ± 160	0.061 ± 0.027	0.130 ± 0.076	0.041 ± 0.003	0.13 ± 0.002	34 ± 6	330 ± 86

[a] Constants were evaluated as in Figure 3. Means and standard errors are from 3–6 experiments.

[b] Denotes moderately nonlinear replots approximated by a straight line.

Table VIb

inhibitor	$\Delta\Delta G_{AChE-BuChE}$ (kcal)	$\Delta\Delta G_{AChE-Y_{337}A}$ (kcal)
edrophonium	−3.5	−1.8
acridine	0.80	1.2
N-methyl-acridinium	0.80	1.6
9-aminoacridine	0.36	1.7
tacrine	0.52	2.0
promazine	2.0	0.18
chlorpromazine	1.5	0.25
promethazine	3.0	1.2
ethopropazine	4.5	4.7

TABLE VIIa DISSOCIATION CONSTANTS AND FREE ENERGY DIFFERENCES FOR THE INHIBITION OF MUTANT ACETYLCHOLINESTERASES BY (-)-HUPERZINE A

	Enzyme	K_1 (μM)	ΔΔG (kcal)[a]
Mouse AChE	Wild Type	0.0085 ± 0.004	0.0
	Tyr337Phe	0.273 ± 0.01	2.1
	Tyr337Ala	8.2 ± 0.1	4.9
Torpedo AChE	Wild Type	0.185 ± 0.01	0.0
	Glu199Gln	0.56 ± 0.07	0.7

[a] Calculated according to the formula ΔΔG = $RT\ln K'_1/K_1$, where K_1 and K'_1 are the dissociation constants for the mutant and wild-type AChE, respectively.

TABLE VIIb-FREE ENERGY DIFFERENCES FOR THE INHIBITION OF CHOLINESTERASES BY THE TWO STEREOISOMERS OF HUPERZINE A

		ΔΔG (k_{cal})[a]		
Enzyme Pair	Mutation	(±)-Hup A	(-)-Hup A	(+)-Hup A
Torpedo-FBS AChE	Phe to Tyr	1.4	2.3	2.8
BuChE-Torpedo AChE	Ala to Phe	3.0	3.2	0.3
BuChE-FBS AChE	Ala to Tyr	4.5	5.4	3.1

[a] Calculated according to the formula ΔΔG = $RT\ln K'_1/K_1$, where K_1 and K'_1 are the dissociation constants for the mutant and wild-type AChE, respectively.

2. Topography of the Acyl Pocket of the Active Center

Studies of the residues in the vicinity of the acyl pocket in mouse AChE reveal that $F_{295(288)}$, $R_{296(289)}$, and $F_{297(290)}$ are the most critical (Tables VIIIa and VIIIb).

These residues have been substituted with L_{295}, S_{296}, I_{297}, the corresponding residues found in BuChE. F_{295} is primarily responsible for governing acyl pocket size and the $F_{295}L$ mutation gives more efficient catalysis of BuTCh than native BuChE (4P). R_{296} is involved in conferring rigidity to the acyl pocket whereas F_{297} is involved in substrate inhibition. The mutation, $F_{297}I$, converts AChE from an enzyme exhibiting substrate inhibition (b = 0.2) to one showing substrate activation (b = 1.8) (Fig. 2). These residue replacements also govern the specificity of BuChE selective organophosphates, like isoOMPA (4P) (Table VIIIa). F_{338} was shown to play a peripheral role in the acyl pocket by virtue of ring stacking.
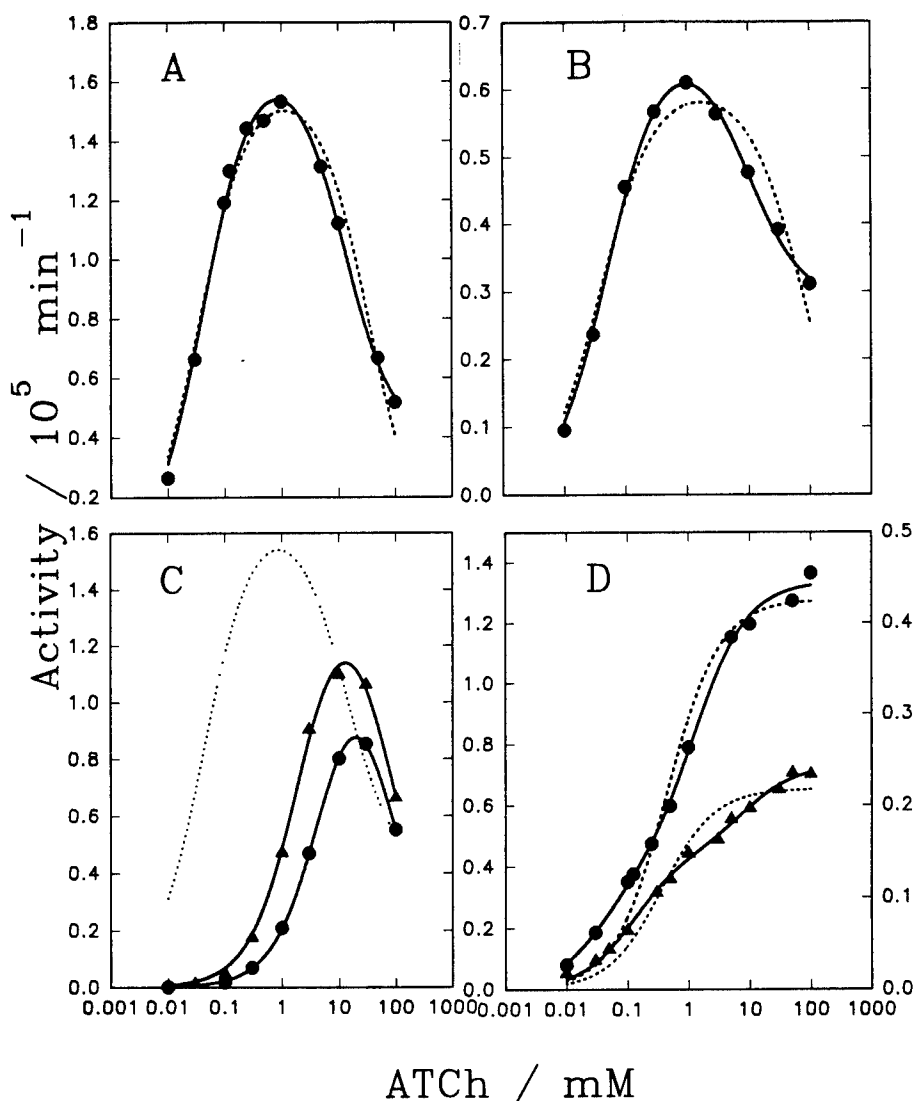

FIGURE 2 Concentration dependencies for acetylcholine hydrolysis by recombinant DNA-derived acetylcholinesterases. Data for wild-type AChE and BuChE are from previously determined concentration dependencies (Vellom et al., 1993). Activities have been normalized to their respective k_{cat} values. (A) Wild-type AChE: - - -, eq 1 (K_m = 39 μM, K_{ss} = 38 mM); —, eq 2 (K_m = 46 μM, K_{ss} = 15 mM, b = 0.23). (B) $Y_{337} \rightarrow F$ mutation: - - -, eq 1 (K_m = 40 μM, K_{ss} = 73 mM); —, eq 2 (K_m = 53 μM, K_{ss} = 10 mM, b = 0.42). (C) Substrate concentration dependencies for mutations substantially diverging from that of wild-type AChE (- - -); $Y_{72}N$, $D_{74}N$, $Y_{124}Q$, $W_{286}A$ (▲); $Y_{72}N$, $D_{74}N$, $Y_{124}Q$, $W_{286}R$ (●). Values for K_m, K_{ss}, and b, which determine the solid lines, are given in Table I. Since K_m and K_{ss} approach each other, note that k_{cat} is greater than the apparent V_{max}. (D) Substrate concentration dependence for BuChE (●): - - -, eq 1 (K_m = 451 μM, K_{ss} = ∞); —, eq 2 (K_m = 35 μM, K_{ss} = 1.3 mM, b = 3.6). $F_{297}I$ mutation (right-hand ordinate scale) (▲): - - -, eq 1 (K_m = 357 μM, K_{ss} = ∞); —, eq 2 (K_m = 172 μM, K_{ss} = 43 mM, b = 1.8).

Table VIIIa Inhibition Constants for the Cholinesterase Chimeras and Site-Directed Mutant Enzymes[a]

chimera/mutant	K_I (BW284c51) (nM)		K_I (ethopropazine) (μM)		k_i (isoOMPA) (M^{-1} min^{-1})
	K_I competitive	αK_I	K_I competitive	αK_I	
AChE		6.5 ± 0.9	≥100		15.9 ± 1.3
BuChE	11300 ± 430	42300 ± 5000	0.062 ± 0.011	0.17 ± 0.03	217000 ± 33000
B$_{5-174}$, A$_{175-575}$	290 ± 80	1600 ± 200	25	50	51 ± 3
B$_{5-174}$, A$_{175-487}$, B$_{488-575}$	707 ± 12	1960 ± 50	43	89	108 ± 15
F$_{295}$ → L		3.1 ± 1.2	≥100		1440 ± 60
R$_{296}$ → S		1.1 ± 1.0	≥100		142 ± 6
F$_{297}$ → I		20 ± 17	44	174	3300 ± 400
V$_{300}$ → G		2.2 ± 0.5	≥100		180 ± 11
F$_{295}$, F$_{297}$ → L, I		19 ± 2	30	111	8500 ± 1250

[a] Inhibition by the reversible inhibitors BW284c51 and ethopropazine was analyzed by construction of reciprocal plots of activity versus substrate concentration. Replots of the slopes and intercepts versus inhibitor concentration yield mixed inhibition from which K_I (competitive) and αK_I are calculated. For ethopropazine, the competitive component is dominant. Standard deviations are derived from the computer-generated replots. No attempt was made to analyze mode of inhibition when K_I exceeded 100 μM. For BW284c51, replots of the slopes for the mutants inhibited at low concentrations do not show linearity, so we did not distinguish the mode of inhibition. k_i for the irreversible inhibitor, isoOMPA, was determined by measuring the rates of inhibition at two isoOMPA concentrations. k_i is directly proportional to inhibitor potency.

Table VIIIb Kinetic Parameters for Cholinesterase Wild-Type and Mutant Enzymes[a]

enzyme	K_m (μM)	K_{ss} (mM)	b	k_{cat} (10^5/min)	k_{cat}/K_m (10^9/min·M)
AChE wt[b]	46 ± 3	15 ± 2	0.23 ± 0.01	1.4 ± 0.1	3.0
BuChE wt[b]	35 ± 2	1.3 ± 0.5	3.6 ± 0.2	0.40 ± 0.07	1.1
Y$_{72}$N	110 ± 20	35 ± 18	0.18 ± 0.13	1.3 ± 0.2	1.2
D$_{74}$N	1300 ± 140	530 ± 170	0	0.84 ± 0.11	0.063
Y$_{124}$Q	120 ± 21	25 ± 13	0.35 ± 0.09	1.1 ± 0.3	0.94
W$_{286}$R	420 ± 60	23 ± 8	0.24 ± 0.06	1.6 ± 0.3	0.38
Y$_{72}$N/Y$_{124}$Q	95 ± 11	21 ± 13	0.65 ± 0.05	0.94 ± 0.20	0.99
Y$_{72}$N/W$_{286}$R	670 ± 200	13 ± 8	0.26 ± 0.05	1.9 ± 0.3	0.28
Y$_{124}$Q/W$_{286}$R	700 ± 170	66 ± 17	0	1.6 ± 0.3	0.23
Y$_{72}$N/Y$_{124}$Q/W$_{286}$R	850 ± 130	10 ± 3	0.24 ± 0.02	2.1 ± 0.6	0.25
Y$_{72}$N/Y$_{124}$Q/W$_{286}$A	230 ± 43	14 ± 6	0.27 ± 0.05	1.5 ± 0.3	0.67
Y$_{72}$N/D$_{74}$N/Y$_{124}$Q/W$_{286}$R	6100 ± 730	75 ± 10	0	1.4 ± 0.2	0.023
Y$_{72}$N/D$_{74}$N/Y$_{124}$Q/W$_{286}$A	2100 ± 300	82 ± 14	0	1.5 ± 0.1	0.071
F$_{295}$Y	17 ± 3	27 ± 9	0	0.061 ± 0.020	0.36
F$_{297}$Y	58 ± 6	460 ± 120	0	0.39 ± 0.13	0.67
Y$_{337}$A	110 ± 16	29 ± 21	0.59 ± 0.08	0.52 ± 0.16	0.46
Y$_{337}$F	53 ± 5	10 ± 2	0.42 ± 0.03	0.68 ± 0.26	1.3
F$_{338}$G	75 ± 9	1300 ± 870	0	0.23 ± 0.10	0.31
B$_{5-174}$A$_{175-575}$[b]	160 ± 2	27 ± 10	0.29 ± 0.06	1.7 ± 0.2	1.0
B$_{5-174}$A$_{175-487}$B$_{488-575}$[b]	160 ± 15	18 ± 8	0.39 ± 0.08	1.2 ± 0.4	0.77
F$_{295}$L[b]	49 ± 4	62 ± 8	0	0.44 ± 0.07	0.90
F$_{297}$I[b]	172 ± 64	43 ± 46	1.8 ± 0.3	0.15 ± 0.02	0.087
R$_{296}$S[b]	50 ± 8	15 ± 4	0.20 ± 0.16	0.92 ± 0.08	1.8
V$_{300}$G[b]	50 ± 4	46 ± 6	0	1.6 ± 0.2	3.2
F$_{295}$L/F$_{297}$I[b]	200 ± 93	83 ± 87	0.67 ± 0.08	0.12 ± 0.01	0.059

[a] Substrate was acetylthiocholine. Values for K_m, K_{ss}, and b were calculated using nonlinear computer fitting . k_{cat} was evaluated using MEPQ titrations . The means and standard errors from 3–5 experiments and 2 different transfections are given. [b] Data of Vellom et al. (1993) .

9

3. The Peripheral Site and the Rim of the Gorge

This region is involved in propidium, fasciculin and *bis*-quaternary inhibitor binding to AChE. It is also believed to be the site of binding of the second substrate molecule producing substrate inhibition (2P). Surprisingly, three residues, W_{286}, Y_{72} and Y_{124}, control all the specificity differences between AChE and BuChE for propidium, BW284c51 and decamethonium (Table IX). Linear free energy partitioning enables one to assess the contributions of the individual side chains (Table X). These residues are conserved in the AChE's but not the BuChE's. D_{74} is also critical in *bis*-quaternary ligand binding, but not in propidium or fasciculin binding. For each of these ligands, differences in free energy of ligand binding with each mutation have been analyzed to examine relationships between residues. The peptide fasciculin also binds to the peripheral anionic site to regulate catalysis. Fasciculin is a weak inhibitor of BuChE, but inhibits AChE with a K_i of 2 pM (Table XI). Interestingly, BuChE inhibition constants can be replicated simply by the $W_{286}R$, $Y_{72}N$, $Y_{124}Q$ substitutions. R, N and Q are found in BuChE at the respective positions.

Table IX Constants (μM) for Reversible Inhibition of Wild-Type AChE and Peripheral Site Mutant Cholinesterases[a]

| | inhibitor | | | | | | | |
| | BW284C51 | | propidium | | decamethonium | | edrophonium | |
enzyme	K_I	αK_I	K_I	αK_I	K_I	αK_I	K_I	αK_I
AChE wt	0.0028 ± 0.0010	0.0048 ± 0.0018	2.2 ± 0.7	5.3 ± 1.8	3.5 ± 1.6	31 ± 16	0.30 ± 0.10	6.4 ± 0.6
BuChE wt	11.3 ± 0.4	42 ± 5	5.3 ± 1.8	26 ± 18	10 ± 1.1	42 ± 25	110 ± 37	1400 ± 700
$Y_{72}N$	0.024 ± 0.009	0.029 ± 0.003	18 ± 5	170 ± 33	22 ± 6	95 ± 22	ND[b]	
$D_{74}N$	1.9 ± 0.4	23 ± 6	8.7 ± 2.1	34 ± 11	830 ± 130	3000 ± 670	ND	
$Y_{124}Q$	0.016 ± 0.002	0.060 ± 0.031	13 ± 6	66 ± 18	26 ± 6	68 ± 2	ND	
$W_{286}R$	0.24 ± 0.08	0.49 ± 0.09	620 ± 170[c]	≥960	390 ± 90	1300 ± 900	ND	
$Y_{72}N/Y_{124}Q$	0.19 ± 0.08	0.46 ± 0.13	35 ± 7	120 ± 44	130 ± 14	510 ± 180	ND	
$Y_{72}N/W_{286}R$	1.6 ± 0.4	2.9 ± 1.1	600 ± 54[c]	1700 ± 1300	1600 ± 500	7700 ± 2500	ND	
$Y_{124}Q/W_{286}R$	3.1 ± 0.1	12 ± 5	1500 ± 360	≥2200	2000 ± 210	6600 ± 2200	ND	
$Y_{72}N/Y_{124}Q/W_{286}R$	16 ± 2	52 ± 20	230 ± 84[c]	470 ± 210	4000 ± 1000	10000 ± 7000	2.1 ± 0.8	12 ± 6
$Y_{72}N/Y_{124}Q/W_{286}A$	4.1 ± 1.8	12 ± 3	230 ± 0	520 ± 190	1300 ± 640	5300 ± 470	1.6 ± 0.3	
$Y_{72}N/D_{74}N/Y_{124}Q/W_{286}R$	780 ± 28	1000 ± 240	1900 ± 760	3200 ± 1600	50000 ± 18000	40000 ± 35000	28 ± 6	
$Y_{72}N/D_{74}N/Y_{124}Q/W_{286}A$	170 ± 6	690 ± 18	1100 ± 430	2700 ± 1200	16000 ± 1000	55000 ± 35000	17 ± 3	≥120

[a] Constants were evaluated   Means and standard errors from 3–5 experiments are given. [b] ND = not determined. [c] Denotes moderately nonlinear replots approximated by a straight line.

Table X   Ratio of Inhibition Constants and Resulting Differences in ΔG for Inhibition by Peripheral Site Inhibitors[a]

| | inhibitor | | | | | |
| | BW284C51 | | deca-methonium | | propidium | |
enzyme	K_I'/K_I	$\Delta\Delta G$ (kcal)	K_I'/K_I	$\Delta\Delta G$ (kcal)	K_I'/K_I	$\Delta\Delta G$ (kcal)
$Y_{72}N$	8.6	1.3	6.2	1.1	8.2	1.3
$Y_{124}Q$	5.7	1.0	7.4	1.2	5.9	1.1
$W_{286}R$	86	2.7	110	2.8	280	3.4
$Y_{72}N/Y_{124}Q$	68	2.5	37	2.2	16	1.7
$Y_{72}N/W_{286}R$	570	3.8	460	3.7	270	3.4
$Y_{124}Q/W_{286}R$	1100	4.2	570	3.8	680	3.9
$B_{5-174}A_{175-575}$	100	2.8	ND[b]	ND	ND	ND
$B_{5-174}A_{175-487}A_{488-575}$	250	3.3	ND	ND	ND	ND
$Y_{72}N/Y_{124}Q/W_{286}R$	5700	5.2	1100	4.2	110	2.8
$Y_{72}N/Y_{124}Q/W_{286}A$	1500	4.4	360	3.5	110	2.8
BuChE	3900	5.0	3.0	0.66	2.4	0.52
$D_{74}N$	680	3.9	240	3.3	4.0	0.83
$Y_{72}N/D_{74}N/Y_{124}N/W_{286}R$	280000	7.5	14000	5.7	860	4.0
$Y_{72}N/D_{74}N/Y_{124}Q/W_{286}A$	59000	6.6	4600	5.1	490	3.7
$Y_{337}A$	5.7	1.0	1.0	0	2.2	0.47

[a] Inhibition constants (K_I') were compared to AChE wt (K_I). Values were derived from the data in Table IX and, in the case of the chimeras, from Vellom et al. (1993). [b] ND = not determined.

Table XI
Dissociation constants for fasciculin with wild-type and mutant acetylcholinesterases, 37 °C

Enzyme	K_i
	pM
AchE (wild type)	2.3 ± 0.7[a]
$F^{295}L$	16 ± 8[a]
$F^{297}I$	57 ± 15[a]
$F^{297}Y$	7.9 ± 1.7[a]
$F^{338}G$	7.9 ± 1.7[a]
$Y^{337}A$	4.2 ± 1.7[a]
$D^{74}N$	43 ± 7[a]
$Y^{124}Q$	248 ± 57[a]
$Y^{72}N$	7,800 ± 900[b]
$W^{286}R$	2,100,000 ± 600,000[c]
$Y^{72}N, Y^{124}Q$	72,000 ± 19,000[b]
$B^{5-174}A^{175-575}$ chimera	91,000 ± 16,000[c]
$Y^{124}Q, W^{286}R$	8,500,000 ± 3,100,000[b]
$Y^{72}N, W^{286}R$	170,000,000 ± 66,000[c]
$Y^{72}N, Y^{124}Q, W^{286}R$	235,000,000 ± 60,000,000[b]
BuChE (wild type)	210,000,000 ± 98,000,000[b]

[a] Mean ± standard error for three or more measurements. Dissociation constants, K_i, were analyzed by the method of Ackerman and Potter after 14–16-h incubations with fasciculin.
[b] Mean values obtained from Lineweaver-Burk and Hunter and Downs plots.
[c] Dissociation constants were analyzed from slopes of double-reciprocal velocity-substrate plots as a function of inhibitor concentration.

4. Molecular Modeling

Our analyses of ligand interactions with cholinesterases contain an essential modeling component and these details are presented in the open literature. In brief, we have used the standard energy minimization docking analysis from standard Biosym programs such as Insight or the more sophisticated dynamics simulations where we conformational movements over a 10-20 psec time frame. We feel fortunate to have access to the San Diego Supercomputer Center on Campus for energy minimization and dynamics simulations. Energy minimization has been used for docking analysis of ligands at the active center and the peripheral anionic site. Dynamics simulations have been used to analyze the conjugate between oxime and the ethyloxy methylphosphonyl enzyme (Section 6). Figure 3 (stereoview) shows a representation of dominant residues in the acyl pocket, choline binding subsite and peripheral site. Figure 4 shows an expanded view of the acyl pocket with acetylcholine associated with the wild-type enzyme and butyrylcholine associated with the $F_{295}L$ mutant.
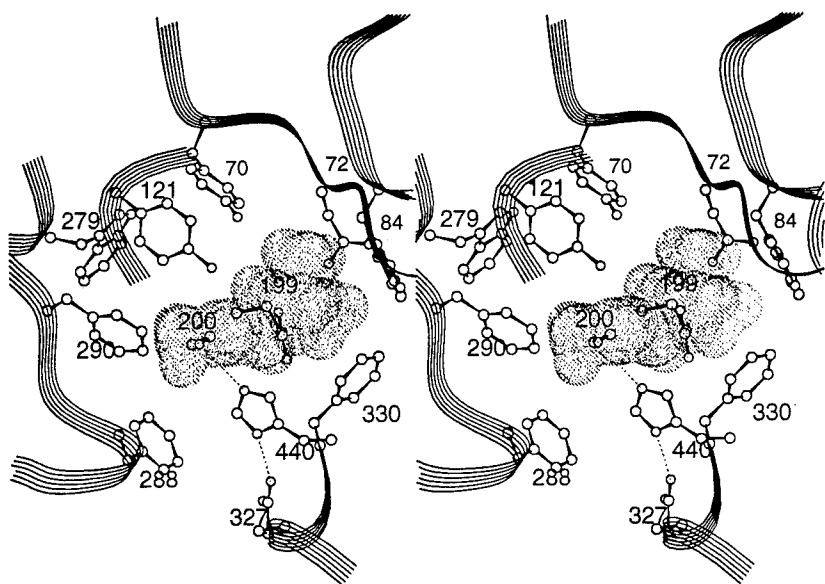
Figure 3 Structure of *Torpedo* acetylcholinesterase showing the positions of critical side chains and bound acetylcholine positioned by energy. (131, 132). (*a*) The catalytic triad: S_{200}, H_{440}, E_{327}. (*b*) The choline binding subsite: W_{84}, Y_{330}, E_{199}. (*c*) The acyl pocket: F_{288}, F_{290}. (*d*) The peripheral anionic site: Y_{70}, Y_{121}, W_{279}, D_{72}.
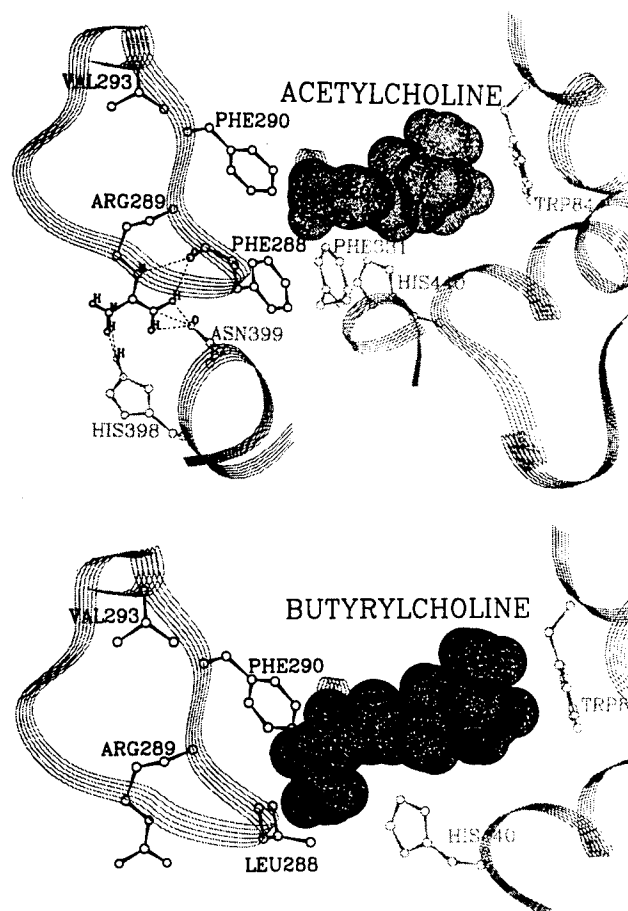
FIGURE 4: Ribbon diagrams of the AChE structure and substrate docked by energy minimization techniques, as described in the test. (Top) Acetylcholine docked to *Torpedo* AChE; (bottom) Butyryl-choline docked to the $F_{288} \rightarrow L$ mutant of *Torpedo* AChE. Side chains subject to mutation are shown in bold type; other landmark side chains are in light type. Hydrogen bonds are shown by the dotted lines.

5. Sites of Membrane Association and Oligomerization

Mutations in the carboxyl-terminal end of the AChE molecule have been directed to understanding the determinants affecting membrane association. To this end we have constructed soluble monomeric, dimeric and tetrameric forms of the molecule, forms which contain a glycophospholipid attachment and forms that are amphiphilic by virtue of containing a domain with a hydrophobic surface. In addition, we have made chimeric forms of AChE in which AChE is linked to transmembrane spanning domains of epidermal growth factor receptor. The expressed species have been characterized with respect to hydrodynamic properties, detergent binding, phospholipase C sensitivity, membrane association and oligomerization. Hence, for each of the three alternatively spliced cDNA's which we have found to exist in mouse and human cells (13,14), we identified the molecular species of AChE produced upon expression in various cell types.

In separate studies we related expression of the molecular species of AChE to message splicing patterns. In this case we transfected genomic DNA into undifferentiated stem, fibroblast, muscle and nerve cells, and analyzed the mRNA species and gene products expressed. These studies are still ongoing but are beginning to reveal the factors controlling cholinesterase splicing and expression during tissue differentiation. Moreover, the secreted monomeric and dimeric forms of AChE can be produced in very high yield. We now have over 80 mg of monomer purified to homogeneity. This material has been provided to the crystallographers in the hope of crystallizing AChE in a distinct conformation.

## 6. Studies of Organophosphate and Oxime Interactions with Acetylcholinesterase

(a) *Organophosphates*: We had initiated studies of organophosphate interactions with the $E_{202(199)}$ mutant early in the project period, but soon realized that this work will be far more complex than anticipated. Accordingly, we asked for an extension of time, but have yet to carry this project to completion. Since the organophosphates contain tetrahedral acyl group, display enantiomeric preferences and are sensitive to the chemistry (pKa) and structure of the leaving group, a comprehensive analysis requires a systematic series of compounds. To this end, we have teamed up with Dr. Harvey Berman at SUNY, Buffalo who has synthesized and rigorously studied a congeneric series of enantiomeric phosphates (15,16).

Our initial studies involved the nonenantiomeric compounds paraoxon and echothiophate (Table XII). We then extended the study to a series of (a) isopropyl methylphosphonates, (b) t-butyl methylphosphonates, and (c) cycloheptyl methyl-phosphonates, all containing thiocholine as a leaving group (Table XIII). Several interesting findings emerge: (1) Stereospecificity is marked for AChE but also is evident for BuChE. (2) Sterospecificity can be reduced or eliminated by modifying F_{295}. This is most marked for the cycloheptyl derivative where the S to R preference can be actually reversed. Since there is substantial evidence that acylation requires the phosphoryl oxygen to be in the oxyanion hole (cf17) it is possible to model the two enantiomers in the active center and ascertain whether steric constraints dictate this preference. This indeed appears to be the case where the F_{295} is critical when the alkyl or alkoxy group exceeds a three carbon length. In addition, our studies point to the thiocholine leaving group assuming a different orientation (presumably toward the gorge exit) than does the thiocholine in the substrate, acetylthiocholine. Collaborative studies with the Walter Reed and USAMRICD groups on soman stereospecificity using several of the same mutants are under way, but have yet to be completed.

Another noteworthy finding is the very different reactivity of human and mouse BuChE toward the organophosphates. This might point to a role for the W_{286} position which exists near the lip of the gorge. The corresponding residue is R in mouse BuChE and A in mouse BuChE. This residue may play a critical role in charge neutralization and
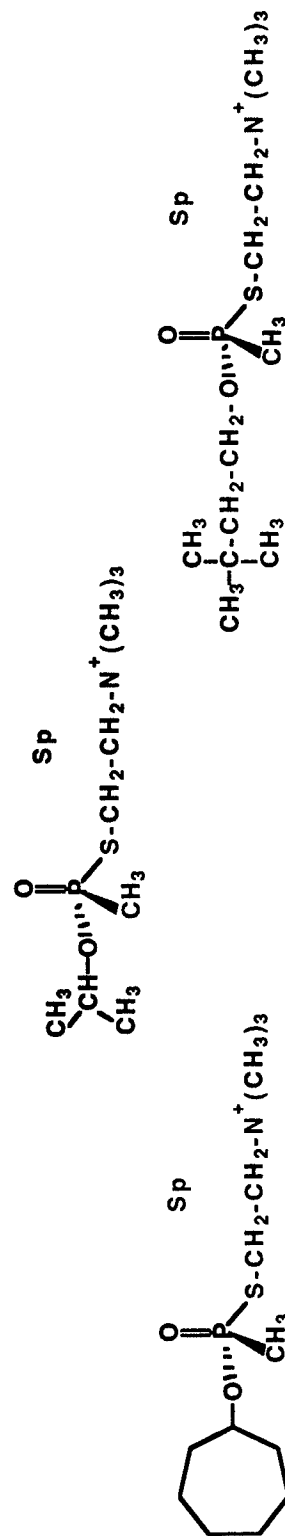
Table XII

Inhibition Summary of Phosphorylation Compounds.

Enzyme Sample	Paraoxon			Echothiophate			MEPQ		
	k_a x10^6/minM	$K_{d(\mu M)}$	$k_{p(min^{-1})}$	k_a x10^6/minM	$K_{d(\mu M)}$	$k_{p(min^{-1})}$	k_a x10^6/minM	$K_{d(\mu M)}$	$k_{p(min^{-1})}$
mAChE	2.0	4.4	8.8	2.1	7.4	15	140	0.12	16
mBuChE	2.6	3.2	9.3	19	1.2	21	400	0.0093	3.9
F295L	28	0.19	5.2	13	0.74	9.9	200	0.050	6.7
F297I	6.5	0.44	2.7	2.1	4.3	8.6	56	0.055	16

Table XIII
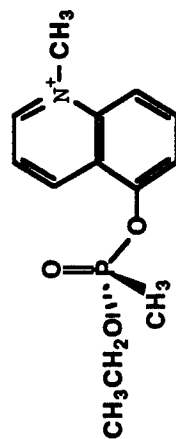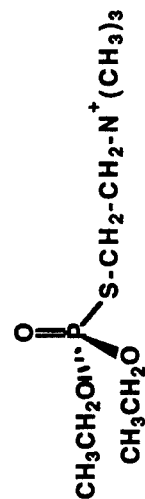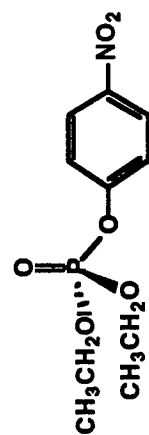
Bimolecular Rate Constants (ka/min^{-1}M^{-1}) of Alkylmethylphosphonylthiocholine Inhibitors with Mutant and Wild-Type Cholinesterases.

Enzyme Sample	Cycloheptylmethyl-			Isopropylmethyl-			3,3-Dimethylbutyl-		
	Sp x10^8	Rp x10^8	Sp/Rp	Sp x10^6	Rp x10^6	Sp/Rp	Sp x10^8	Rp x10^8	Sp/Rp
mAChE	1.5	0.0072	208	15	0.1	150	3.5	0.28	12.5
tAChE	(3.0)	(0.014)	(220)	(13)	(0.087)	(149)	(10)	(0.33)	(31)
mBuChE	4.4	0.063	70	9.1	3.3	2.8	5.2	0.42	12.3
hBuChE	0.074	0.00081	91	0.16	0.034	4.7	0.94	0.077	12.2
F295L	0.73	0.076	9.6	3.3	1.2	2.8	1.3	0.17	7.6
F297I	0.093	0.58	0.16	5.8	1.5	3.9	0.25	0.22	1.1

( ) = Data obtained from ref: Berman & Leonard, JBC 264(7), 1989; Enzyme species was *Torpedo* AChE.

positioning the thiocholine containing phosphonates in the productive complex. A series of neutral phosphothioates have also been studied (Table XIV). We have also analyzed some of the reactions in more depth where the bimolecular rate constant for organophosphate acylation, k_a, has been deconstructed into an equilibrium dissociation constant, K_D, and a unimolecular reaction rate constant, k_p, (Tables XV, XVI and XVII). As is evident from the tables, this work is incomplete. A major reason for this is that many of the reaction rates are too fast for conventional measurements and we will have to go to stopped-flow measurements to see a limiting reaction rate at high organophosphate concentrations. We feel that completion of this work is essential to a comprehensive analysis of organophosphate reaction mechanisms and specificity.

   (b) *Aging*: In conjunction with Ashima Saxena and B.P. Doctor at Walter Reed, and with Donald Maxwell and David Lenz at the Aberdeen Proving Ground [UCAMR-ICD], we have found that modification of $E_{202(199)}$ to the neutral glutamine changes the pH dependence for organophosphate aging and effectively makes these cholinesterases susceptible to oxime reactivation (8P).

   (c) *Oxime Reactivation of the Cholinesterases*: In conjunction with Yacov Ashani and B.P. Doctor at Walter Reed, we have examined the residues involved in oxime reactivation of organophosphate-AChE complexes. To this end we have employed methyl ethoxyphosphinyloxy-1-methylquinolinium iodide (MEPQ) to phosphonylate the enzyme. By using stoichiometric quantities, we have been able to achieve approximately an equal ratio of the two enantiomic O-ethylmethylphosphonyl conjugates (R and S). Reactivation rates are primarily controlled by the charged residue $E_{202(199)}$ for its conversion to glutamine reduced rates by 16- to 33-fold. Suprisingly, the residues W86 and Y337 showed little involvement in the reactivation process. We also observe different rates of reactivation for the R and S enantiomers and show a potential mechanism wherein one of the enantiomers is preferred due to stabilization of the phosphonyl oxygen in the oxyanion hole (19P) (Tables XVIII and XIX). Finally we show that the enhanced efficacy of HI-6 over 2-PAM as a reactivating agent stems from the additional stabilization energy conferred by interaction of the extended chain of HI-6 with key amino acid residues (W286, Y124, Y72, D74) at the entry to the active center gorge. Such an approach should enable one to develop antidotes with a higher degree of selectivity.

Table XIV

Summary of Bimolecular Rate Constants (ka, min^{-1}M^{-1}) for Alkylmethylphosphonyl Thiocholines & Thioates with Butyrylcholinesterases

Alkyl-MP Thio Compound	Mouse BuChE			Human BuChE			MBu/HBu		
	S x 10^6	R x 10^6	S/R	S x 10^6	R x 10^6	S/R	S/S	R/R	$\frac{S/R}{S/R}$
Isopropyl-MP thiocholine	9.1	3.3	2.8	0.16	0.034	4.7	56	97	0.6
Dimethylbutyl-MP thiocholine	520	42	12	94	7.7	12.2	5.5	5.5	1.0
Cycloheptyl-MP thiocholine	440	6.3	70	7.4	0.081	91	59	78	0.8
Cycloheptyl-MP S-methyl-thioate	0.23	0.0018	130	0.029	0.00042	69	7.9	4.3	1.9
Cycloheptyl-MP S-ethyl-thioate	0.13	0.0015	87	0.044	0.00010	440	3.0	15	0.2

Table XV

Cycloheptylmethylphosphonothioate Inhibition Summary

S-methyl(R)

Enzyme Sample	k_a (min⁻¹M⁻¹)			K_d (µM)			k_p (min⁻¹)		
	Sp x10⁵	Rp x10⁵	Sp/Rp	Sp	Rp	Sp/Rp	Sp	Rp	Sp/Rp
mAChE	3.1	0.011	280	30	>>100	<0.3	9.3	>0.11	<85
mBuChE	2.3	0.018	130	16	99	0.16	3.7	0.18	21
hBuChE	0.29	0.0042	69	80	31	2.6	2.3	0.013	175
F295L	3.4	0.018	190	99	>>100	<1	34	>0.18	<190
F297I	0.52	0.185	2.8	440	91	4.8	23	1.7	13

S-ethyl(R)

Enzyme Sample	k_a (min⁻¹M⁻¹)			K_d (µM)			k_p (min⁻¹)		
	Sp x10⁵	Rp x10⁵	Sp/Rp	Sp	Rp	Sp/Rp	Sp	Rp	Sp/Rp
mAChE	0.76	0.0019	400	250	>>100	<2.5	19	>0.019	<1000
mBuChE	1.3	0.015	87	78	110	0.71	10	0.17	59
hBuChE	0.44	0.0010	440	64	63	1.0	2.8	0.0063	440
F295L	1.6	0.0075	210	>>20	180	>0.11	>3.2	0.14	>23
F297I	0.67	0.21	3.2	175	109	1.6	12	2.3	5.2
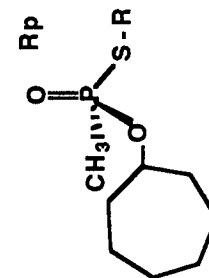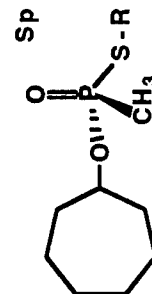
Table XVI

Isopropylmethylphosphonyl Thiocholine Inhibition Summary

Enzyme Sample	k_a (min^{-1}M^{-1})			K_d (µM)			k_p (min^{-1})		
	Sp x10^6	Rp x10^6	Sp/Rp	Sp	Rp	Sp/Rp	Sp	Rp	Sp/Rp
mAChE tAChE	15 (13)	0.1 (0.087)	150 (149)	»0.12† (9.3)	»20 (110)	na (0.08)	>1.8 (117)	>2 (9)	na (13)
mBuChE	9.1	3.3	2.8	»0.24	»1	na	>2.2	>3.3	na
hBuChE	0.16	0.034	4.7	»4.8	45	>0.11	>0.77	1.5	>0.51
F295L	3.3	1.2	2.8	»0.6	6.4	>0.09	>2.0	7.7	>0.26
F295A	17	nd	na	»0.1	nd	na	>1.7	nd	na
F297I	0.58	1.5	3.9	14	0.87	16	8.1	1.3	6.2
F297A	1.7	nd	na	»1	nd	na	>1.7	nd	na
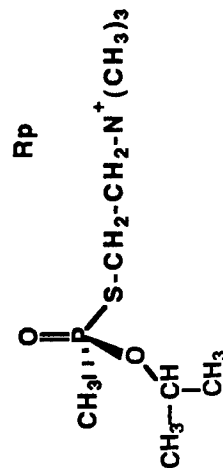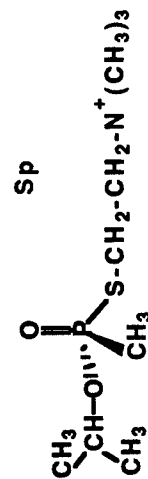
( ) = Data obtained from ref: Berman & Leonard, JBC 264(7), 1989; Enzyme species was *Torpedo* AChE.
† = refers to much greater than the highest concentration of inhibitor used.
na = not applicable
nd = not determined

Table XVII

3,3-Dimethylbutylmethylphosphonyl Thiocholine Inhibition Summary

Enzyme Sample	k_a (min⁻¹M⁻¹)			K_d (µM)			k_p (min⁻¹)		
	Sp x10⁸	Rp x10⁸	Sp/Rp	Sp	Rp	Sp/Rp	Sp	Rp	Sp/Rp
mAChE	3.5	0.28	13	»0.01†	0.39	>0.03	>3.5	11	>0.32
tAChE	(10)	(0.33)	(31)	(0.28)	(2.9)	(0.096)	(311)	(95)	(3.3)
mBuChE	5.2	0.42	12	»0.01	0.17	>0.06	>5	5.3	>0.94
hBuChE	0.94	0.077	12	0.33	»0.1	<3.3	31	>0.77	<40
F295L	1.3	0.17	7.6	»0.03	0.81	>0.04	>3.9	14	>0.28
F295A	4.9	nd	na	»0.01	nd	na	>4.9	nd	na
F297I	0.13	0.055	2.4	»0.1	»0.1	na	>1.3	>0.55	na
F297A	0.55	nd	na	»0.1	nd	na	>5.5	nd	na

( ) = Data obtained from ref: Berman & Leonard, JBC 264(7), 1989; Enzyme species was *Torpedo* AChE.
† = refers to much greater than the highest concentration of inhibitor used.
na = not applicable
nd = not determined

Table XVIII Biochemical Parameters for the Binding of 2-PAM to ChE and the Reactivation of $EMP_{R,S}$-ChEs by 2-PAM[a]

Enzyme	K_α[b] (mM)	K'_α[c] (mM)		k'_{max}[c] (min⁻¹)		k_r X10²[d] (M⁻¹min⁻¹)		$k_{oximate}$ X10²[e] (M⁻¹min⁻¹)	
		fast	slow	fast	slow	fast	slow	fast	slow
MAChE wt	0.049 (±0.007)	0.18 (±0.08)	0.57 (±0.38)	0.093 (±0.010)	0.028 (±0.006)	5.2	0.49	14.9	1.40
W86A	ND[f]	0.26 (±0.11)	0.62 (±0.20)	0.11 (±0.01)	0.013 (±0.002)	4.2	0.21	12.0	0.60
W86F	0.297	NR[g]	NR	NR	NR	3.8[h] (±0.6)	0.21[h] (±0.02)	10.9	0.60
Y337F	0.086	0.29 (±0.11)	0.58 (±0.38)	0.22 (±0.04)	0.039 (±0.017)	7.6	0.67	21.7	1.92
Y337A	0.357	0.60 (±0.27)	1.75 (±0.63)	0.36 (±0.05)	0.054 (±0.012)	6.0	0.31	17.2	0.88
E202Q	0.172 (±0.038)	0.82 (±0.23)	2.86 (±1.08)	0.013 (±0.001)	0.006 (±0.003)	0.16	0.021	0.45	0.06
F295L	0.141	0.27 (±0.04)	0.17 (±0.06)	0.038 (±0.002)	0.007 (±0.001)	1.4	0.41	4.0	1.17
W286R	0.132 ±0.018	0.077 (±0.049)	0.17 (±0.08)	0.036 (±0.004)	0.014 (±0.002)	4.7	0.82	13.4	2.35
W286A Y72N Y124Q	0.229 (±0.021)	0.73 (±0.37)	1.16 (±0.45)	0.23 (±0.04)	0.019 (±0.003)	3.2	0.16	9.2	0.46
TAChE	0.089 (±0.008)	0.40 (±0.12)	0.96 (±0.64)	0.39 (±0.09)	0.029 (±0.007)	9.8	0.30	28.0	0.86
HBUChE	ND	1.59 (±0.28)	1.35 (±0.66)	0.58 (±0.04)	0.009 (±0.001)	3.6	0.07	10.3	0.20

[a]P2S (2-Pam) in 25 mM phosphate, pH 7.8, 25°C.
[b]Mean ± SEM (n=4 determinations). Values without SEM are average from two determinations
(4-5 data points each) that differ <30%.
[c]Obtained from nonlinear regression analysis of the data points. Figures in parentheses are SE (n=5-12).
[d]Obtained by dividing k'_{max} by K'_{ox}.
[e]Normalized to oximate anion concentration at pH 7.8.
[f]Not determined.
[g]Individual constants sould not be resolved.
[h]Calculated from the slope of the line obtained by plot of k_{obs} against [P2S].

Table XIX   Parameters for the Binding of HI-6 to ChE and the Reactivation of $EMP_{R,S}$-ChEs by HI-6 [a]

Enzyme	K_{ox} [b] (mM)	K'_{ox} [c] (mM)		k'_{max} [c] (min^{-1})		k_r X10^2 [d] (M^{-1}min^{-1})		$k_{oximate}$ X10^2 [e] (M^{-1}min^{-1})	
		fast	slow	fast	slow	fast	slow	fast	slow
MAChE Wt	0.013 (±0.002)	0.066 (±0.017)	0.071 (±0.045)	0.25 (±0.02)	0.0250 (±0.007)	37.9	3.5	55.7	5.2
W86A	ND [f]	0.45 (±0.11)	NR [g]	0.77 (±0.13)	NR	17.1	0.68 [h] (±0.08)	25.1	1.0
Y337A	0.108 [i]	0.095 (±0.032)	0.067 (±0.032)	0.53 (±0.12)	0.0175 (±0.006)	55.8	2.6	82.0	3.8
E202Q	0.0134 (±0.004)	0.045 (±0.029)	0.091 (±0.063)	0.011 (±0.002)	0.0024 (±0.0006)	2.4	0.26	3.5	0.4
F295L	0.0125	0.080 (±0.038)	0.051 (±0.018)	0.66 (±0.21)	0.091 (±0.019)	82.5	17.8	121.3	26.2
W286R	ND	NR	0.29 (±0.02)	NR	0.021 (±0.003)	0.94 [h] (±0.08)	0.72	1.4	1.1
W286A Y72N Y124Q	0.085 (±0.011)	0.57 (±0.15)	0.091 (±0.020)	0.031 (±0.003)	0.0055 (±0.0004)	0.54	0.60	0.79	0.9
HBUChE	ND	NR	NR	NR	NR	1.47 [h] (±0.04)	0.076 [h] (±0.011)	2.16	0.1

[a]25 mM phosphate, pH 7.8, 25°. [b]Mean ± SEM (n=4 determinations). Values without SEM are averages from two determinations (4-5 data points each) that differ 30%. [c]Obtained from nonlinear regression analysis of the data. Figures in parentheses are SE (n=5-12). [d]Obtained by dividing k'_{max} by K'_{ox}. [e]Normalized to oximate anion concentration at pH 7.8. [f]Not defined. [g]Individual constants could not be resolved. [h]Calculated from the slope of the line obtained by plot of k_{obs} against [HI-6].

D. Publications: (Listed below are publications supported in full or in part by the DAMDC contract. Other publications from the laboratory on expression and gene structure of AChE and BuChE facilitated our progress with the contract objectives, but they were primarily supported by NIH funds.)

Publications: July 1991 - Present:
Original Articles:

1P. Ogert, R.A., Gentry, M.K., Richardson, E.C., Deal, C.D., Abramson, S.N., Alving, C.R., Taylor, P. and Doctor, B.P. Studies on the Topography of the Catalytic Site of Acetylcholinesterase Using Polyclonal and Monoclonal Antibodies. J. Neurochem. 55:756-763 (1991).

2P. Radić, Z., Reiner, E. and Taylor, P. Role of the Peripheral Anionic Site on Acetylcholinesterase: Inhibition by Substrates and Coumarin Derivatives. Molecular Pharmacol. 39:98-104 (1991).

3P. Radić, Z., Gibney, G., McPhee-Quigley, K., Kawamoto, S., Bongiorno, C. and Taylor, P. Expression of Recombinant Acetylcholinesterase in Baculovirus Systems: Kinetic Properties of Glutamate 199 Mutants. Biochemistry 31: 9760-9767 (1992).

4P. Vellom, D.C., Radić, Z., Li, Y., Pickering, N.A., Camp, S, and Taylor, P. Amino Acid Residues Controlling Acetylcholinesterase and Butyrylcholinesterase Specificity. Biochemistry 32:12-17 (1993).

5P. Radić, Z., Pickering, N., Vellom, D.C., Camp, S. and Taylor, P. Three Distinct Domains in the Cholinesterase Molecule Confer Selectivity for Acetyl- and Butyrylcholinesterase Inhibitors. Biochemistry. 32: 12074-12084 (1993).

6P. Radić, Z., Duran, R., Cervalenski, C., Vellom, D.C., Li, Y. and Taylor, P. Site of Fasciculin Interaction with Acetylcholinesterase. J. Biol. Chem. 269: 11233-11239 (1994).

7P. Wasserman, L., Doctor, B.P., Gentry, M.K. and Taylor, P. Epitope Mapping of Form Specific and Nonspecific Antibodies to Acetylcholinesterases. J. Neurochem. 61:2124-2143 (1993).

8P. Saxena, A., Doctor, B.P., Maxwell, D.M., Lenz, D.E., Radić, Z. and Taylor, P. The Role of Glutamate 199 in the Aging of Cholinesterase. Biochem. Biophys. Res. Comm. 197:343-349 (1993).

9P. Saxena, A., Qian, N., Kovach, I.M., Kozikowski, A.P., Vellom, D.C. Radić, Z., Taylor, P. and Doctor, B.P. (1994) Identification of Amino Acid Residues Involved in the Binding of Huperzine-A Enantiomers to Cholinesterases. Protein Science (in press).

10P. Taylor, P., Gibney, G., Camp, S., Maulet, Y., Ekström, T., Rachinsky, T. and Li, Y. Features of Acetylcholinesterase Structure and Gene Expression Emerging from Recent Recombinant DNA Studies. Proc. Third Int. Conference on Cholinesterases, J. Massoulie, J.P. Toutant, D. Quinn and B.P. Doctor (eds.), ACS Books, Washington, DC, pp. 179-185 (1991).

11P. Taylor, P. Cholinesterases. minireview, J. Biol. Chem. 266:4025-4028 (1991).

12P. Taylor, P., Li, Y., Camp, S., Rachinsky, T.L. and Getman, D. Acetylcholinesterase Gene Expression and Organization. in: Current Research in Alzheimer Therapy. Giacobini, E. and Becker, R. (eds) Birkhäuser, Boston, pp. 53-62 (1991).

13P. Taylor, P., Li, Y., Camp, S., Kawamoto, S., Rachinsky, T., Getman, D. and Radić, Z. Structure and Regulation of Expression of the Acetylcholinesterase Gene. Proceedings Third Int. Conference on Esterases, E. Reiner (ed.), Chem. Biol. Interactions 87: 199-207 (1993).

14P. Massoulie, J., Sussman, J., Doctor, B.P., Soreq, H., Velan, B., Cygler, M., Rotundo, R., Shafferman, A., Silman, I. and Taylor, P. Recommendations for Nomenclature on Cholinesterases. Proc. 36th Oholo Conference, A. Shafferman & B. Velan (eds.), Plenum, NY, pp. 285-288 (1992).

15P. Taylor, P. Impact of Recombinant DNA Technology and Protein Structure Determination on Past and Future Studies on Acetylcholinesterase, Plenary Lecture, Proceedings 36th Oholo Conference, A. Shafferman & B. Velan (eds.), Plenum Press, NY, pp.1-15 (1992).

16P. Taylor, P., Li, Y., Camp, S., Radić, Z., Getman, D., Rachinsky, T.L., Ekström, T.L., Fuentes, M.E., Kawamoto, S., Vellom, D.C. and Pickering, N.A. Acetylcholinesterase: Regulation of Expression of its Gene and Modification of Enzyme Structure. Proceedings 4th Yokohama International Medical Seminar, Yokohama Medical Bulletin. 43:146-157 (1992).

17P Taylor, P. and Radić, Z. The Cholinesterases: From Genes to Proteins. Ann. Rev. Pharmacol. Toxicol. 34:281-320 (1994).

18P Quinn, D.M., Seravalli, J., Nair, H.K., Radić, Z., Vellom, D.C., Pickering, N.A and Taylor, P. Electrostatic Influence on Acylation Reaction Dynamics of Acetylcholinesterase Catalysis, Biochemistry (in press).

19P Ashani, Y., Radić, Z., Tsigelny, I., Vellom, D.C., Pickering, N.A., Quinn, D.M., Doctor, B.P. and Taylor, P. Amino Acid Residues Controlling Reactivation of a Chiral Organophosphonyl Conjugates of Acetylcholinesterase by Mono- and Bisquaternary Oximes, J. Biol. Chem. (in press).

E.   Personnel Supported by Contract
Palmer Taylor, Ph.D., Daniel Vellom, Ph.D., Natilie Pickering, B.S., Zoran Radić, Ph.D., Shelley Camp, M.A., Ying Li, M.D., Ph.D., Tara Rachinsky, Ph.D.

CONCLUSIONS

These studies have made important inroads into: (a) obtaining mammalian cholinesterases in amounts sufficient for detailed studies of the behavior of mutant enzymes, (b) demonstrating the kinetic sophistication necessary for generating data on mutant enzymes that will be of archival value, (c) demonstrating the role of the acyl pocket, choline binding site and peripheral anionic site in dictating substrate and inhibitor binding specificity, (d) partially deconstructing the catalytic parameters, k_{cat} and K_m, to analyze how inhibitors influence access to the gorge (i.e., diffusion), the commitment to catalysis [the ratio of enzyme acylation to substrate dissociation, i.e., $(k_2/k_2 + k_1)$] and deacylation rates, (e) analysis of the stereospecificity and selectivity of the organophosphate reaction and the residues dictating acylation and aging rates, (f) analysis of the specificity of oxime reactivation in terms of stereospecificity of oxime reactivation in terms of stereospecificity of the organophosphate and binding of the respective oxime (2-PAM or HI-6).

REFERENCES

1)   Sussman, J.L., Harel, M., Frolow, F., Oefner, C., Goldman, A., et al. 1991. Atomic structure of acetylcholinesterase from Torpedo californica: a prototypic acetylcholine-binding protein. Science 253:872-79.

2)   Schumacher, M., Camp, S., Maulet, Y., Newton, M., MacPhee-Quigley, K., et al., 1986. Primary structure of Torpedo california acetylcholinesterase deduced from cDNA sequences. Nature 319:407-9.

3)   MacPhee-Quigley, K., Vedvick, T.S., Taylor, P., Taylor, S.S. 1986. Profile of disulfide bonds in acetylcholinesterase. J. Biol. Chem. 261:13565-70.

4)   MacPhee-Quigley, K., Taylor, P., Taylor, S.S. 1985. Primary structures of catalytic subunits from two molecular forms of acetylcholinesterase: a comparison of NH2-terminal and active center sequences. J. Biol. Chem. 260:12185-89.

5)   Gibney, G., MacPhee-Quigley, K., Thompson, B., Vedvick, T., Low, M.G. et al., 1988. Divergence in primary structure between molecular forms of acetylcholinesterase. J. Biol. Chem.263:1140-45.

6)   Gibney, G., Camp, S., Dionne, M., MacPhee-Quigley, K., Taylor, P. 1990. Mutagenesis of essential functional residues in acetylcholinesterase. Proc. Natl. Acad. Sci. USA 87:7546-50.

7) Rachinsky, T.L., Camp, S., Li, Y., Ekstrom, T.J., Newton, M. Taylor, P. 1990. Molecular cloning of mouse acetylcholinesterase: tissue distribution of alternatively spliced mRNA species. *Neuron* 5:317-27.

8) Maulet, Y., Camp, S., Gibney, G., Rachinsky, T.L., Ekstrom, T.J., Taylor, P. 1990. A single gene encodes glycophospholipid-anchored and asymmetric acetylcholinesterase forms: alternative coding exons contain inverted repeat sequence. *Neuron* 4:289-301.

9) Li, Y., Camp, S., Rachinsky, T.L., Getman, D.K., Taylor, P. 1991. Gene structure of mammalian acetylcholinesterase: alternative exons dictate tissue-specific expression. *J. Biol. Chem.* 266:22083-90.

10) Li, Y., Camp, S., Taylor, P. 1993. Tissue-specific expression and alternative mRNA processing of the mammalian acetylcholinesterase gene. *J. Biol. Chem.* 268:5790-97.

11) Li, Y., Camp, S., Rachinsky, T.L., Bongiorno, C., Taylor, P. 1993. Promoter elements and transcriptional control of the mouse acetylcholinesterase gene. *J. Biol. Chem.* 268:3563-72.

12) Harel, M., Schalk, I., Ehret-Sabatier, L., Bouet, F., Goeldner, M., et al. 1993. Quaternary ligand binding site of acetylcholinesterase as revealed by X-ray crystallography and photoaffinity labeling. *Proc. Natl. Acad. Sci USA.* 90:9031-35.

13) Camp, S., Bon, S., Li, Y., Getman, D.K., Engel, A.G., Massoulie, J., Taylor, P. 1995. Patients with congenital myasthenia associated with end-plate acetylcholinesterase deficiency show normal sequence, mRNA splicing and assembly of catalytic subunits. *J. Clin. Inv.* 95:333-340.

14) Vellom, D.K., Camp, S., Taylor, P. 1994. Relationship of gene structure to the expression of the molecular species of acetylcholinesterase (submitted for publication).

15) Berman, H.A., Leonard, K. 1989. Chiral reactions of acetylcholinesterase probed with enantiomeric methylphosphonothioates. *J. Biol. Chem.* 214:3942-50.

16) Berman, H.A., Decker, M.M. 1989. Chiral nature of covalent methylphosphonyl conjugates of acetylcholinesterase. *J. Biol. Chem.* 264:3951-3956.

17) Cygler, M., Grochulski, P., Kazlauskas, R.J., Schrag, J.D., Bouthillier, F., Rubin, B., Serreqi, A.N., Gupta, A.K. 1994. A structural basis for the chiral preferences of lipases. *J. Amer. Chem. Soc.* 116:3180-3186.